

1 2 3 4 1 **Transcriptional mapping of the primary somatosensory cortex upon sensory deprivation**

5
6 2 Koen Kole^{1,2}, Yutaro Komuro¹, Jan Provaznik³, Jelena Pistolic³,

7
8 3 Vladimir Benes³, Paul Tiesinga², Tansu Celikel¹

9
10 4 (1) Department of Neurophysiology, (2) Department of Neuroinformatics, Donders Institute for
11 5 Brain, Cognition, and Behaviour, Radboud University, Nijmegen - the Netherlands. (3) European
12 6 Molecular Biology Laboratory (EMBL), Genomics Core Facility, Heidelberg - Germany

13
14 7 E-mail addresses (in the order of appearance): k.kole@neurophysiology.nl,
15 8 y.komuro@neurophysiology.nl, jan.provaznik@embl.de, jelena.pistollic@embl.de,
16 9 benes@embl.de, p.tiesinga@science.ru.nl, celikel@neurophysiology.nl (corresponding author)

18 19 10 20 11 **Background (138)**

22 12 Experience-dependent plasticity (EDP) is essential for anatomical and functional maturation of
23 13 sensory circuits during development. Although the principal synaptic and circuit mechanisms of
24 14 EDP are increasingly well studied experimentally and computationally, its molecular mechanisms
25 15 remain largely elusive. EDP can be readily studied in the rodent barrel cortex, where each 'barrel
26 16 column' preferentially represents deflections of its own principal whisker. Depriving select
27 17 whiskers while sparing their neighbours introduces competition between barrel columns,
28 18 ultimately leading to weakening of intracortical, translaminal (i.e. Cortical Layer (L)4-to-L2/3) feed-
29 19 forward excitatory projections in the deprived columns. The same synapses are potentiated in the
30 20 neighbouring spared columns. These experience-dependent alterations of synaptic strength are
31 21 thought to underlie somatosensory map plasticity. We used RNA sequencing in this model system
32 22 to uncover cortical-column and -layer specific changes on the transcriptome level that are induced
33 23 by altered sensory experience.

34 24 **Findings (66)**

35 25 Column- and layer-specific barrel cortical tissues were collected from juvenile mice with all
36 26 whiskers intact and mice that received 11-12 days long whisker (C-row) deprivation before high
37 27 quality RNA was purified and sequenced. The current dataset entails an average of 50 million
38 28 paired-end reads per sample, 75 base pairs in length. On average, 90.15% of reads could be
39 29 uniquely mapped to the mm10 reference mouse genome.

40 30 **Conclusions (32) – Word total for the abstract: 246 out of 250**

41 31 The current data reveal the transcriptional changes in gene expression in the barrel cortex upon
42 32 altered sensory experience in juvenile mice and will help to molecularly map the mechanisms of
43 33 cortical plasticity.

44
45
46
47
48
49
50
51
52
53
54
55
56
57
58
59
60
61
62
63
64
65

1
2
3
4
5
6
7
8
9
10
11
12
13
14
15
16
17
18
19
20
21
22
23
24
25
26
27
28
29
30
31
32
33
34
35
36
37
38
39
40
41
42
43
44
45
46
47
48
49
50
51
52
53
54
55
56
57
58
59
60
61
62
63
64
65

34 **Data Description**

35 **Context**

36 Sensory experience powerfully shapes neural circuits. Changes due to sensory organ deprivation
37 such as eye closure, digit amputation, and whisker trimming provide powerful means for studying
38 mechanisms of experience dependent cortical plasticity.

39 In the whisker system experience dependent plasticity is most commonly studied in the
40 barrel cortex subfield of the primary somatosensory cortex where neural representations of
41 whiskers change in response to altered patterns of incoming sensory information. As originally
42 shown in the barrel cortex [1] sensory deprivation induced by transient whisker trimming is
43 sufficient to perturb neural receptive fields both during development and in adulthood. Previous
44 work has also shown that the cellular basis of deprivation-induced decreases in whisker evoked
45 representations are primarily due to a reduction of synaptic strength in monosynaptically
46 connected feed-forward neuronal networks in behaving animals [2, 3]. Conversely whisker
47 sparing induced enhancement in whisker representation is mediated at least in part by the long-
48 term synaptic facilitation expressed along the L4 projections *in vivo* [4]. Identification of the
49 molecular events that mediate these bidirectional changes in synaptic connectivity will benefit
50 from systematic analysis of the gene transcription. Therefore, we performed RNA sequencing in
51 the barrel cortex with or without sensory deprivation across cortical layers 2-4. This database will
52 assist molecular and cellular neurobiologists in addressing the molecular mechanisms associated
53 with experience dependent plasticity, and will enable statistical approaches to determine the
54 dynamics of the coupled changes across molecular pathways as cortical circuits undergo plastic
55 changes in their organization.

56

1
2
3
4
5
6
7
8
9
10
11
12
13
14
15
16
17
18
19
20
21
22
23
24
25
26
27
28
29
30
31
32
33
34
35
36
37
38
39
40
41
42
43
44
45
46
47
48
49
50
51
52
53
54
55
56
57
58
59
60
61
62
63
64
65

57 **Methods**

58 *Animals*

59 All experiments were performed in accordance with the Animal Ethics Committee of the Radboud
60 University in Nijmegen, the Netherlands. Pregnant wild type mice (Charles River, stock number
61 000664) [RRID:NCBITaxon_10090] were kept at a 12-hour light/dark cycle with access to food
62 *ad libitum*. Cages were checked for birth daily. To induce experience-dependent plasticity, pups
63 underwent bilateral plucking of their C-row whiskers under isoflurane anaesthesia at P12 (**Figure**
64 **1**). Control animals were not plucked but anaesthetized and handled similarly. After recovery pups
65 were returned to their home cage. Every other day pups were checked for whisker regrowth,
66 which were plucked if present. At P23-P24, pups were randomly selected from their litter for slice
67 preparation and tissue collection. For each experimental condition (i.e. whisker deprived or
68 control), 4 female pups were used, thus each group consisted of 4 independent biological samples
69 (also known as biological replicates). Samples from cortical layer (L) 4 and L2/3 were treated
70 independently with their own corresponding groups of control, deprived, 1st order spared, 2nd order
71 spared columns as detailed in Figure 1.

72
73 *Figure 1 is about here*
74

75 *Slice preparation and sample collection*

76 Pups were anaesthetized using isoflurane and then perfused with ice-cold carbogenated slicing
77 medium (108 mM ChCl, 3 mM KCl, 26 mM NaHCO₃, 1.25 mM NaH₂PO₄, 25 mM glucose, 1 mM
78 CaCl₂, 6 mM MgSO₄ and 3 mM Na-pyruvate). Next, pups were decapitated before the brain was
79 quickly dissected out and 400 µm thalamocortical slices from each hemisphere were prepared as
80 described before [2, 3]. Slices were transferred to 37 degrees Celsius carbogenated ACSF (120
81 mM NaCl, 3.5 mM KCl, 10 mM glucose, 2.5 mM CaCl₂, 1.3 mM MgSO₄, 25 mM NaHCO₃ and 1.25

1
2
3
4 82 mM NaH₂PO₄) where they were kept for 30 minutes and recovered at room temperature for
5
6 83 another 30 minutes until tissue collection.

7
8
9 84

10 85 After incubation, slices were placed under a Nikon Eclipse FN1 microscope. The holding chamber
11
12
13 86 was continuously perfused with room temperature carbogenated ACSF. Due to the 55 degree
14
15 87 cut, slices were obtained in which S1 barrels from specific rows (A-E) could be identified [2]. A
16
17 88 thin, long glass pipette was pulled using a Sutter instruments P-2000 pipette puller and was used
18
19 89 to make intercolumnar incisions from L1 to the bottom of L4 after which the slice was placed under
20
21
22 90 a binocular dissection microscope where the location of specific barrel columns could now be
23
24 91 readily identified by eye. A sterile 32G needle was then used to cut out L2/3 and L4 separately
25
26 92 from each column. Tissue from columns A/E and B/D were pooled as they both constitute second
27
28 93 and first order spared whiskers, respectively. Immediately after dissection, tissue samples were
29
30 94 snap frozen in liquid nitrogen and stored at -80 degrees Celsius until further use. All tools that
31
32
33 95 came into direct contact with brain tissue were treated using RNaseZap in order to minimize
34
35 96 RNase contamination.

36
37
38 97

39 40 98 *RNA isolation and quality control*

41
42 99 Tissue samples originating from the same rows and layers were pooled within each animal. From
43
44 100 control animals, only the C column tissues were used (also see *Re-use potential*). Tissue was
45
46 101 quickly dissolved in Qiazol (Qiagen #79306), after which RNA was isolated using the miRNeasy
47
48 102 Mini kit (Qiagen #217004), DNase treated (Thermo Scientific, #EN0521) and cleaned up using
49
50 103 RNeasy MinElute kit (Qiagen #74204), all following the manufacturer's instructions. Samples were
51
52
53 104 then stored at -80 degrees Celsius until further processing.

54
55
56 105

57
58 106 RNA sample integrity was determined using Agilent Tapestation (High Sensitivity RNA
59
60 107 Screentape). Sample RINs ranged from 7.1 to 8.8. To further assess RNA purity and integrity,

61
62
63
64
65

1
2
3
4 108 RNA samples were used in RT-PCR to confirm that cDNA could be produced and that a large
5
6 109 (~1000 bp) amplicon could be obtained. To produce cDNA, SuperScript® II Reverse
7
8 110 Transcriptase (Thermo Scientific #18064014) and random hexamer primers (Roche
9
10 111 #11034731001) were used. The resulting cDNA was then added to a PCR reaction mix which
11
12
13 112 further consisted of Jumpstart Ready Mix (Sigma P2893) and exon-exon junction spanning
14
15 113 CamKII primers (FW TCCAACATTGTACGCCTCCAT; RV TGTTGGTGCTGTCGGAAGAT).
16
17 114 From all cDNA samples a fragment of the expected size could be amplified, suggesting that the
18
19 115 RNA samples contained pure RNA of sufficient integrity. All RNA samples thus passed our quality
20
21
22 116 control criteria and were subjected to RNA sequencing.

23
24 117
25
26 118 *RNA sequencing*

27
28 119 RNA sequencing was conducted at the Genomics Core Facility of the EMBL, Heidelberg,
29
30
31 120 Germany [RRID:SCR_004473]. The cDNA library was generated using the non-stranded
32
33 121 NEBNext Ultra RNA Library Preparation Kit for Illumina (New England Biolabs, catalogue
34
35 122 #E7530), which includes oligo-dT bead selection of mRNA. For library enrichment, 13-14 PCR
36
37 123 cycles were performed. Pooled libraries were sequenced on the Illumina NextSeq 500 instrument
38
39 124 [RRID:SCR_014983] in a 75bp paired-end mode using High output flow cells.

40
41 125
42
43
44 126 **Data validation and quality control**

45
46 127 Sequencing read quality was assessed using FastQC (Babraham Bioinformatics)
47
48 128 [RRID:SCR_014583], the results of which were merged using MultiQC (<http://multiqc.info>)
49
50 129 [RRID:SCR_014982]. Results are displayed in **Figure 2**. Per base quality *phred* scores range
51
52 130 from 34.80 to 35.15, indicating base call accuracies of >99.9% (**Figure 2A**). Overall 91.48-94.03%
53
54 131 of reads had a mean *phred* score of 30 or above (**Figure 2B**). In line with these scores, per base
55
56 132 N content (i.e. percentage of bases that could not confidently called) was very low, with a
57
58 133 maximum value 0.053%.

1
2
3
4 134
5
6 135
7
8 136
9
10
11 137
12
13 138
14
15 139
16
17 140
18
19 141
20
21 142
22
23 143
24
25 144
26
27 145
28
29 146
30
31 147
32
33 148
34
35 149
36
37 150
38
39 151
40
41 152
42
43 153
44
45 154
46
47 155
48
49 156
50
51 157
52
53 158
54
55 159
56
57
58
59
60
61
62
63
64
65

Figure 2 is about here

Reads were then mapped to the mm10 reference genome using STAR [5] [RRID:SCR_005622], which uniquely mapped between 39,000,000 and 59,000,000 reads, constituting an average 90.15% unique map rate across samples (**Figure 2D**). Since the library preparation protocol entails a PCR enrichment step, which can lead to technical duplication and hence an overestimation of observed transcripts, we used Seqmonk (Babraham Bioinformatics) [RRID:SCR_001913] to plot the read density against the duplication levels (i.e. the percentage of duplicate reads) for each transcript. The obtained duplication plots showed a clear positive relation between read density and duplication levels (**Figure 3** and **Supplemental Figure 1**), suggesting that the origin of read duplication is biological, rather than technical. Based on the above quality control measures we determined that our RNA-sequencing data was of sufficient quality to be used in downstream analyses, therefore we continued with gene expression analysis.

Figure 3 is about here

Analysis of gene expression

Using a 2 read cut-off we identified 16,900 to 17,600 transcripts per sample (**Figure 4A**). Raw gene counts can be found online (see Supporting Data – DOI to appear). Differential gene expression analyses across groups were performed using EdgeR v3.12.1 [6, 7] [RRID:SCR_012802] using only genes with a count per million (CPM) >1 in at least 4 samples (**Supplementary Table 1** for details on the commands used). Since laminar identity is an important feature of our experimental setup, we assessed the relative expression of known

1
2
3
4 160 molecular markers for L2/3 (*Cacna1h*, *Id2*, *Igfbp4*, *Igfn1*, *Mdga1*, *Plcx1*, *Rasgrf2*, *Rgs8*, *Tle3*)
5
6 161 and L4 (*Cartpt*, *Cyp39a1*, *Kcnh5*, *Kcnip2*, *Lmo3*, *Rorb*, *Scnn1a*) [8–10], which showed selective
7
8 162 enrichment of the laminar markers in isolated layers (**Figure 4B**).

10
11 163
12
13 164 *Figure 4 is about here*

14
15 165
16
17 166 To assess the variance in transcript counts, we calculated the coefficient of variation (CV) for
18
19 167 each transcript with a cut-off of 50 as the minimal read count separately for each group (**Figure**
20
21 168 **4C**). This analysis showed that, on average, 85.93% of transcripts have a CV below 15%,
22
23 169 suggesting low variance across transcript counts for individual genes. Principal component
24
25 170 analysis (PCA) showed that samples cluster based on layer, and the first two components
26
27 171 explained ~88% variance the data (**Figure 4C, Supplemental Figure 2B**).

28
29 172
30
31 173 These quality control routines suggest that we have obtained RNA-sequencing data of high read
32
33 174 quality, with individual bases being called confidently throughout the length of reads, which
34
35 175 uniquely map to the mm10 reference genome at high rates (>90% average). The laminar origin
36
37 176 of our samples could be identified through known molecular markers, confirming our samples are
38
39 177 of high anatomical specificity.
40
41
42
43

44 178 45 46 179 **Re-use potential**

47
48
49 180 The current RNA-seq dataset might help address the molecular underpinnings of cortical
50
51 181 experience-dependent plasticity. For example, it could be used (1) to identify genes whose
52
53 182 transcription is modulated in an experience-dependent manner, (2) to statistically map the
54
55 183 transcriptional networks at laminar resolution, (3) creating synergy with the single neuron RNA-
56
57 184 seq datasets [11, 12], to address the molecular diversity of the cortical networks, (4) combined
58
59 185 with the proteomic analysis performed under comparable experimental conditions in the
60
61
62
63
64
65

1
2
3
4
5
6
7
8
9
10
11
12
13
14
15
16
17
18
19
20
21
22
23
24
25
26
27
28
29
30
31
32
33
34
35
36
37
38
39
40
41
42
43
44
45
46
47
48
49
50
51
52
53
54
55
56
57
58
59
60
61
62
63
64
65

186 accompanying manuscript (Kole et al, submitted), to systematically study the transcriptional and
187 translational regulation of the genome upon altered sensory experience, and finally (5) to identify
188 and quantify splice isoforms, given the sequencing depth of the current dataset. Since splicing
189 and other posttranscriptional mechanisms govern which proteins are ultimately produced,
190 combining the current transcriptomic dataset with a proteomics approach would also be of high
191 importance.

192
193 The current dataset focuses on isolated cortical columns and layers, which are necessarily
194 diverse samples containing neuronal and non-neuronal cell classes. In terms of experience
195 dependent plasticity, although most previous studies focus on excitatory projections, inhibitory
196 cells and even non-neuronal cells have been implicated in plasticity [13–15]. This heterogeneity
197 might be particularly important for L2/3, as also shown by the principal component analysis
198 (**Figure 4D**), given the relative diversity of cellular populations in supragranular layers and their
199 heterogeneous connectivity patterns [16].

200
201 Researchers reusing our dataset should be aware that comparisons between control column C
202 and spared columns (A/E, B/D) may have to be approached with caution, as this would involve
203 two different columnar identities (whose transcriptomic dissimilarities are currently unknown),
204 each coming from cortices that have had different sensory experience. However direct
205 comparisons between the C columns across experimental conditions (i.e control versus deprived)
206 as well as within-animal across-column comparisons in deprived animals control for these
207 confounding variables.

208
209 Taken together we hope that this data will prove useful in discovering novel molecular targets
210 responsible for cortical plasticity and will lead to targeted control of plasticity in health and disease.

211

References

1. Hand PJ (1892) Plasticity of the rat cortical barrel system. In: Strick P, Morrison AD (eds) *Changing concepts of the nervous system*. Academic Press, New York, pp 49–75
2. Allen CB, Celikel T, Feldman DE (2003) Long-term depression induced by sensory deprivation during cortical map plasticity in vivo. *Nat Neurosci* 6:291–9. doi: 10.1038/nn1012
3. Celikel T, Szostak VA, Feldman DE (2004) Modulation of spike timing by sensory deprivation during induction of cortical map plasticity. *Nat Neurosci* 7:534–41. doi: 10.1038/nn1222
4. Clem RL, Celikel T, Barth AL (2008) Ongoing in vivo experience triggers synaptic metaplasticity in the neocortex. *Science* 319:101–4. doi: 10.1126/science.1143808
5. Dobin A, Davis CA, Schlesinger F, Drenkow J, Zaleski C, Jha S, Batut P, Chaisson M, Gingeras TR (2013) STAR: ultrafast universal RNA-seq aligner. *Bioinformatics* 29:15. doi: 10.1093/bioinformatics/bts635
6. Robinson MD, McCarthy DJ, Smyth GK (2010) edgeR: a Bioconductor package for differential expression analysis of digital gene expression data. *Bioinformatics* 26:139. doi: 10.1093/bioinformatics/btp616
7. McCarthy DJ, Chen Y, Smyth GK (2012) Differential expression analysis of multifactor RNA-Seq experiments with respect to biological variation. *Nucleic Acids Res* 40:4288. doi: 10.1093/nar/gks042
8. Molyneaux BJ, Goff LA, Rinn JL, Arlotta P (2015) Genome-wide Analysis of In Vivo Transcriptional Dynamics during Pyramidal Neuron Fate Selection in Neocortex *NeuroResource DeCoN: Genome-wide Analysis of In Vivo Transcriptional Dynamics during Pyramidal Neuron Fate Selection in Neocortex*. 275–288.
9. Xue M, Atallah B V., Scanziani M (2014) Equalizing excitation–inhibition ratios across visual cortical neurons. *Nature* 511:596–600. doi: 10.1038/nature13321
10. Rowell JJ, Mallik AK, Dugas-Ford J, Ragsdale CW (2010) Molecular analysis of neocortical layer structure in the ferret. *J Comp Neurol* 518:3272–3289. doi: 10.1002/cne.22399
11. Zeisel A, Munoz-Manchado AB, Codeluppi S, Lonnerberg P, La Manno G, Jureus A, Marques S, Munguba H, He L, Betsholtz C, Rolny C, Castelo-Branco G, Hjerling-Leffler J, Linnarsson S (2015) Cell types in the mouse cortex and hippocampus revealed by single-cell RNA-seq. *Science* (80-) 347:1138–1142. doi: 10.1126/science.aaa1934
12. Tasic B, Menon V, Nguyen TN, Kim TK, Jarsky T, Yao Z, Levi B, Gray LT, Sorensen SA, Dolbeare T, Bertagnolli D, Goldy J, Shapovalova N, Parry S, Lee C, Smith K, Bernard A, Madisen L, Sunkin SM, Hawrylycz M, Koch C, Zeng H (2016) Adult mouse cortical cell taxonomy revealed by single cell transcriptomics. *Nat Neurosci* 19:335–346. doi: 10.1038/nn.4216
13. Tropea D, Van Wart A, Sur M (2009) Molecular mechanisms of experience-dependent plasticity in visual cortex. *Philos Trans R Soc Lond B Biol Sci* 364:341–55. doi: 10.1098/rstb.2008.0269
14. Kole K (2015) Experience-dependent plasticity of neurovascularization. *J Neurophysiol* 114:2077–9. doi: 10.1152/jn.00972.2014
15. Foeller E, Celikel T, Feldman DE (2005) Inhibitory sharpening of receptive fields contributes to whisker map plasticity in rat somatosensory cortex. *J Neurophysiol* 94:4387–400. doi: 10.1152/jn.00553.2005
16. Markram H, Muller E, Ramaswamy S, Reimann MW, Abdellah M, Sanchez CA, Ailamaki A, Alonso-Nanclares L, Antille N, Arsever S, Kahou GAA, Berger TK, Bilgili A, Buncic N, Chalimourda A, Chindemi G, Courcol J-D, Delalondre F, Delattre V, Druckmann S, Dumusc R, Dynes J, Eilemann S, Gal E, Gevaert ME, Ghobril J-P, Gidon A, Graham JW, Gupta A, Haenel V, Hay E, Heinis T, Hernando JB, Hines M, Kanari L, Keller D, Kenyon

1
2
3
4
5
6
7
8
9
10
11
12
13
14
15
16
17
18
19
20
21
22
23
24
25
26
27
28
29
30
31
32
33
34
35
36
37
38
39
40
41
42
43
44
45
46
47
48
49
50
51
52
53
54
55
56
57
58
59
60
61
62
63
64
65

263 J, Khazen G, Kim Y, King JG, Kisvarday Z, Kumbhar P, Lasserre S, Le Bé J-V,
264 Magalhães BRC, Merchán-Pérez A, Meystre J, Morrice BR, Muller J, Muñoz-Céspedes
265 A, Muralidhar S, Muthurasa K, Nachbaur D, Newton TH, Nolte M, Ovcharenko A,
266 Palacios J, Pastor L, Perin R, Ranjan R, Riachi I, Rodríguez J-R, Riquelme JL, Rössert
267 C, Sfyraakis K, Shi Y, Shillcock JC, Silberberg G, Silva R, Tauheed F, Telefont M, Toledo-
268 Rodriguez M, Tränkler T, Van Geit W, Díaz JV, Walker R, Wang Y, Zaninetta SM,
269 DeFelipe J, Hill SL, Segev I, Schürmann F (2015) Reconstruction and Simulation of
270 Neocortical Microcircuitry. *Cell* 163:456–492. doi: 10.1016/j.cell.2015.09.029
271

1
2
3
4
5
6
7
8
9
10
11
12
13
14
15
16
17
18
19
20
21
22
23
24
25
26
27
28
29
30
31
32
33
34
35
36
37
38
39
40
41
42
43
44
45
46
47
48
49
50
51
52
53
54
55
56
57
58
59
60
61
62
63
64
65

272 Availability of the supporting data

273 Supporting data are available online (<https://goo.gl/tBof51>) and will be distributed via GigaScience
274 DB.

275 Raw sequence reads were deposited in NCBI GEO.

276 Link: <https://www.ncbi.nlm.nih.gov/geo/query/acc.cgi?acc=GSE90929>

278 List of abbreviations

279 EDP Experience dependent plasticity

280 L2/3 Cortical Layer 2/3, also known as supragranular layers

281 L4 Cortical Layer 4, i.e. granular layer

283 Competing interests

284 The authors declare no competing interests.

286 Author contributions

287 KK performed all experimental manipulations, sample acquisition, biological and bioinformatic
288 quality controls, and prepared the tables and figures. YK and JaP performed bioinformatic
289 analysis. JeP performed library prep. VB supervised RNA-seq. PT contributed bioinformatic
290 analysis and co-supervised the project. TC designed and supervised the project. KK and TC wrote
291 the manuscript. All authors edited otherwise approved the final version of the manuscript.

1
2
3
4 **292 Figure Legends**

5 **293**
6 **294** **Figure 1.** Overview of the experimental design, sample collection and data organization. **(A)** Pups
7 **295** were bilaterally spared or deprived of off their C-row whiskers between P12 and P23-P24, when
8 **296** acute slices are made and column- and layer-specific tissues were excised. **(B)** RNA was isolated,
9 **297** checked for integrity and purity, and subsequently sequenced. **(C)** Organization of the database.
10 **298** Colour codes denote experimental groups. Same denominations are used in the read counts
11 **299** matrix file (see **Supplemental Data**).
12
13
14

15 **300**
16 **301** **Figure 2.** FastQC and STAR output graphs for all samples. **(A-B)** *Phred* scores per base and
17 **302** per sequence. **(C)** Per sequence GC content. **(D)** STAR output of alignment scores.
18 **303**

19 **304** **Figure 3.** Overlays of duplication plot contours, showing a positive correlation between read
20 **305** density and duplication levels. Depicted contours enclose 90% of the data points.
21 **306**

22 **307** **Figure 4.** Gene expression analyses. **(A)** Histogram of read counts per transcript per sample.
23 **308** With a cut-off of 2 reads, between 16,900 and 17,600 transcripts could be identified across
24 **309** samples. **(B)** Relative expression of known molecular markers for cortical laminae. Layer 4
25 **310** markers are enriched in samples originating from this layer; the same is true for Layer 2/3 marker
26 **311** expression in Layer 2/3 samples. **(C)** Cumulative plots of the coefficient of variance (CV) of
27 **312** individual experimental groups. Including only transcripts identified by 50 reads or more, average
28 **313** CVs of <15% are found in ~85% of transcripts. **(D)** Principal component analysis (PCA) showing
29 **314** sample clustering by layer, including only transcripts identified by at least 50 reads. Principal
30 **315** component (PC) 1 and 2 account for 88% of overall variance.
31 **316**

32 **317** **Supplemental Figure 1.** Duplication plots for all samples, produced using SeqMonk (Babraham
33 **318** Bioinformatics).
34 **319**

35 **320** **Supplemental Figure 2.** **(A)** Cumulative plots of the coefficient of variance (CV) of experimental
36 **321** each group, including transcripts identified by at least one read. Average CVs of <25% are
37 **322** found in ~85% of transcripts. **(B)** Principal component analysis (PCA) including transcripts
38 **323** identified by at least one read. The majority (88%) of overall variance is explained by Principal
39 **324** components (PC) 1 and 2.
40
41
42
43
44
45
46
47
48
49
50
51
52
53
54
55
56
57
58
59
60
61
62
63
64
65

1 2 3 4 1 **Transcriptional mapping of the primary somatosensory cortex upon sensory deprivation**

5
6 2 Koen Kole^{1,2}, Yutaro Komuro¹, Jan Provaznik³, Jelena Pistolic³,

7
8 3 Vladimir Benes³, Paul Tiesinga², Tansu Celikel¹

9
10 4 (1) Department of Neurophysiology, (2) Department of Neuroinformatics, Donders Institute for
11 5 Brain, Cognition, and Behaviour, Radboud University, Nijmegen - the Netherlands. (3) European
12 6 Molecular Biology Laboratory (EMBL), Genomics Core Facility, Heidelberg - Germany

13
14 7 E-mail addresses (in the order of appearance): k.kole@neurophysiology.nl,
15 8 y.komuro@neurophysiology.nl, jan.provaznik@embl.de, jelena.pistollic@embl.de,
16 9 benes@embl.de, p.tiesinga@science.ru.nl, celikel@neurophysiology.nl (corresponding author)

10 11 **Background (138)**

12 Experience-dependent plasticity (EDP) is essential for anatomical and functional maturation of
13 13 sensory circuits during development. Although the principal synaptic and circuit mechanisms of
14 14 EDP are increasingly well studied experimentally and computationally, its molecular mechanisms
15 15 remain largely elusive. EDP can be readily studied in the rodent barrel cortex, where each 'barrel
16 16 column' preferentially represents deflections of its own principal whisker. Depriving select
17 17 whiskers while sparing their neighbours introduces competition between barrel columns,
18 18 ultimately leading to weakening of intracortical, translaminal (i.e. Cortical Layer (L)4-to-L2/3) feed-
19 19 forward excitatory projections in the deprived columns. The same synapses are potentiated in the
20 20 neighbouring spared columns. These experience-dependent alterations of synaptic strength are
21 21 thought to underlie somatosensory map plasticity. We used RNA sequencing in this model system
22 22 to uncover cortical-column and -layer specific changes on the transcriptome level that are induced
23 23 by altered sensory experience.

24 **Findings (66)**

25 Column- and layer-specific barrel cortical tissues were collected from juvenile mice with all
26 26 whiskers intact and mice that received 11-12 days long whisker (C-row) deprivation before high
27 27 quality RNA was purified and sequenced. The current dataset entails an average of 50 million
28 28 paired-end reads per sample, 75 base pairs in length. On average, 90.15% of reads could be
29 29 uniquely mapped to the mm10 reference mouse genome.

30 **Conclusions (32) – Word total for the abstract: 246 out of 250**

31 The current data reveal the transcriptional changes in gene expression in the barrel cortex upon
32 32 altered sensory experience in juvenile mice and will help to molecularly map the mechanisms of
33 33 cortical plasticity.

1
2
3
4
5
6
7
8
9
10
11
12
13
14
15
16
17
18
19
20
21
22
23
24
25
26
27
28
29
30
31
32
33
34
35
36
37
38
39
40
41
42
43
44
45
46
47
48
49
50
51
52
53
54
55
56
57
58
59
60
61
62
63
64
65

1
2
3
4
5
6
7
8
9
10
11
12
13
14
15
16
17
18
19
20
21
22
23
24
25
26
27
28
29
30
31
32
33
34
35
36
37
38
39
40
41
42
43
44
45
46
47
48
49
50
51
52
53
54
55
56
57
58
59
60
61
62
63
64
65

34 **Data Description**

35 **Context**

36 Sensory experience powerfully shapes neural circuits. Changes due to sensory organ deprivation
37 such as eye closure, digit amputation, and whisker trimming provide powerful means for studying
38 mechanisms of experience dependent cortical plasticity.

39 In the whisker system experience dependent plasticity is most commonly studied in the
40 barrel cortex subfield of the primary somatosensory cortex where neural representations of
41 whiskers change in response to altered patterns of incoming sensory information. As originally
42 shown in the barrel cortex [1] sensory deprivation induced by transient whisker trimming is
43 sufficient to perturb neural receptive fields both during development and in adulthood. Previous
44 work has also shown that the cellular basis of deprivation-induced decreases in whisker evoked
45 representations are primarily due to a reduction of synaptic strength in monosynaptically
46 connected feed-forward neuronal networks in behaving animals [2, 3]. Conversely whisker
47 sparing induced enhancement in whisker representation is mediated at least in part by the long-
48 term synaptic facilitation expressed along the L4 projections *in vivo* [4]. Identification of the
49 molecular events that mediate these bidirectional changes in synaptic connectivity will benefit
50 from systematic analysis of the gene transcription. Therefore, we performed RNA sequencing in
51 the barrel cortex with or without sensory deprivation across cortical layers 2-4. This database will
52 assist molecular and cellular neurobiologists in addressing the molecular mechanisms associated
53 with experience dependent plasticity, and will enable statistical approaches to determine the
54 dynamics of the coupled changes across molecular pathways as cortical circuits undergo plastic
55 changes in their organization.

56

1
2
3
4 **Methods**

5
6 *Animals*

7
8
9 All experiments were performed in accordance with the Animal Ethics Committee of the Radboud
10 University in Nijmegen, the Netherlands. Pregnant wild type mice (Charles River, [stock number](#)
11 [000664](#)) [[RRID:NCBITaxon_10090](#)]- were kept at a 12-hour light/dark cycle with access to food
12
13 *ad libitum*. Cages were checked for birth daily. To induce experience-dependent plasticity, pups
14
15
16
17
18
19
20
21
22
23
24
25
26
27
28
29
30
31
32
33
34
35
36
37
38
39
40
41
42
43
44
45
46
47
48
49
50
51
52
53
54
55
56
57
58
59
60
61
62
63
64
65
66
67
68
69
70
71
72
73
74
75
76
77
78
79
80
81
82
83
84
85
86
87
88
89
90
91
92
93
94
95
96
97
98
99
100
101
102
103
104
105
106
107
108
109
110
111
112
113
114
115
116
117
118
119
120
121
122
123
124
125
126
127
128
129
130
131
132
133
134
135
136
137
138
139
140
141
142
143
144
145
146
147
148
149
150
151
152
153
154
155
156
157
158
159
160
161
162
163
164
165
166
167
168
169
170
171
172
173
174
175
176
177
178
179
180
181
182
183
184
185
186
187
188
189
190
191
192
193
194
195
196
197
198
199
200
201
202
203
204
205
206
207
208
209
210
211
212
213
214
215
216
217
218
219
220
221
222
223
224
225
226
227
228
229
230
231
232
233
234
235
236
237
238
239
240
241
242
243
244
245
246
247
248
249
250
251
252
253
254
255
256
257
258
259
260
261
262
263
264
265
266
267
268
269
270
271
272
273
274
275
276
277
278
279
280
281
282
283
284
285
286
287
288
289
290
291
292
293
294
295
296
297
298
299
300
301
302
303
304
305
306
307
308
309
310
311
312
313
314
315
316
317
318
319
320
321
322
323
324
325
326
327
328
329
330
331
332
333
334
335
336
337
338
339
340
341
342
343
344
345
346
347
348
349
350
351
352
353
354
355
356
357
358
359
360
361
362
363
364
365
366
367
368
369
370
371
372
373
374
375
376
377
378
379
380
381
382
383
384
385
386
387
388
389
390
391
392
393
394
395
396
397
398
399
400
401
402
403
404
405
406
407
408
409
410
411
412
413
414
415
416
417
418
419
420
421
422
423
424
425
426
427
428
429
430
431
432
433
434
435
436
437
438
439
440
441
442
443
444
445
446
447
448
449
450
451
452
453
454
455
456
457
458
459
460
461
462
463
464
465
466
467
468
469
470
471
472
473
474
475
476
477
478
479
480
481
482
483
484
485
486
487
488
489
490
491
492
493
494
495
496
497
498
499
500
501
502
503
504
505
506
507
508
509
510
511
512
513
514
515
516
517
518
519
520
521
522
523
524
525
526
527
528
529
530
531
532
533
534
535
536
537
538
539
540
541
542
543
544
545
546
547
548
549
550
551
552
553
554
555
556
557
558
559
560
561
562
563
564
565
566
567
568
569
570
571
572
573
574
575
576
577
578
579
580
581
582
583
584
585
586
587
588
589
590
591
592
593
594
595
596
597
598
599
600
601
602
603
604
605
606
607
608
609
610
611
612
613
614
615
616
617
618
619
620
621
622
623
624
625
626
627
628
629
630
631
632
633
634
635
636
637
638
639
640
641
642
643
644
645
646
647
648
649
650
651
652
653
654
655
656
657
658
659
660
661
662
663
664
665
666
667
668
669
670
671
672
673
674
675
676
677
678
679
680
681
682
683
684
685
686
687
688
689
690
691
692
693
694
695
696
697
698
699
700
701
702
703
704
705
706
707
708
709
710
711
712
713
714
715
716
717
718
719
720
721
722
723
724
725
726
727
728
729
730
731
732
733
734
735
736
737
738
739
740
741
742
743
744
745
746
747
748
749
750
751
752
753
754
755
756
757
758
759
760
761
762
763
764
765
766
767
768
769
770
771
772
773
774
775
776
777
778
779
780
781
782
783
784
785
786
787
788
789
790
791
792
793
794
795
796
797
798
799
800
801
802
803
804
805
806
807
808
809
810
811
812
813
814
815
816
817
818
819
820
821
822
823
824
825
826
827
828
829
830
831
832
833
834
835
836
837
838
839
840
841
842
843
844
845
846
847
848
849
850
851
852
853
854
855
856
857
858
859
860
861
862
863
864
865
866
867
868
869
870
871
872
873
874
875
876
877
878
879
880
881
882
883
884
885
886
887
888
889
890
891
892
893
894
895
896
897
898
899
900
901
902
903
904
905
906
907
908
909
910
911
912
913
914
915
916
917
918
919
920
921
922
923
924
925
926
927
928
929
930
931
932
933
934
935
936
937
938
939
940
941
942
943
944
945
946
947
948
949
950
951
952
953
954
955
956
957
958
959
960
961
962
963
964
965
966
967
968
969
970
971
972
973
974
975
976
977
978
979
980
981
982
983
984
985
986
987
988
989
990
991
992
993
994
995
996
997
998
999
1000

Figure 1 is about here

75 *Slice preparation and sample collection*

76 Pups were anaesthetized using isoflurane and then perfused with ice-cold carbogenated slicing
77 medium (108 mM ChCl, 3 mM KCl, 26 mM NaHCO₃, 1.25 mM NaH₂PO₄, 25 mM glucose, 1 mM
78 CaCl₂, 6 mM MgSO₄ and 3 mM Na-pyruvate). Next, pups were decapitated before the brain was
79 quickly dissected out and 400 µm thalamocortical slices from each hemisphere were prepared as
80 described before [2, 3]. Slices were transferred to 37 degrees Celsius carbogenated ACSF (120
81 mM NaCl, 3.5 mM KCl, 10 mM glucose, 2.5 mM CaCl₂, 1.3 mM MgSO₄, 25 mM NaHCO₃ and 1.25

1
2
3
4 82 mM NaH₂PO₄) where they were kept for 30 minutes and recovered at room temperature for
5
6 83 another 30 minutes until tissue collection.

7
8
9 84

10 85 After incubation, slices were placed under a Nikon Eclipse FN1 microscope. The holding chamber
11
12
13 86 was continuously perfused with room temperature carbogenated ACSF. Due to the 55 degree
14
15 87 cut, slices were obtained in which S1 barrels from specific rows (A-E) could be identified [2]. A
16
17 88 thin, long glass pipette was pulled using a Sutter instruments P-2000 pipette puller and was used
18
19
20 89 to make intercolumnar incisions from L1 to the bottom of L4 after which the slice was placed under
21
22 90 a binocular dissection microscope where the location of specific barrel columns could now be
23
24 91 readily identified by eye. A sterile 32G needle was then used to cut out L2/3 and L4 separately
25
26 92 from each column. Tissue from columns A/E and B/D were pooled as they both constitute second
27
28 93 and first order spared whiskers, respectively. Immediately after dissection, tissue samples were
29
30 94 snap frozen in liquid nitrogen and stored at -80 degrees Celsius until further use. All tools that
31
32
33 95 came into direct contact with brain tissue were treated using RNaseZap in order to minimize
34
35 96 RNase contamination.

36
37
38 97

39 40 98 *RNA isolation and quality control*

41
42 99 Tissue samples originating from the same rows and layers were pooled within each animal. From
43
44 100 control animals, only the C column tissues were used (also see *Re-use potential*). Tissue was
45
46 101 quickly dissolved in Qiazol (Qiagen #79306), after which RNA was isolated using the miRNeasy
47
48 102 Mini kit (Qiagen #217004), DNase treated (Thermo Scientific, #EN0521) and cleaned up using
49
50 103 RNeasy MinElute kit (Qiagen #74204), all following the manufacturer's instructions. Samples were
51
52
53 104 then stored at -80 degrees Celsius until further processing.

54
55
56 105

57
58 106 RNA sample integrity was determined using Agilent TapeStation (High Sensitivity RNA
59
60 107 Screentape). Sample RINs ranged from 7.1 to 8.8. To further assess RNA purity and integrity,

61
62
63
64
65

1
2
3
4 108 RNA samples were used in RT-PCR to confirm that cDNA could be produced and that a large
5
6 109 (~1000 bp) amplicon could be obtained. To produce cDNA, SuperScript® II Reverse
7
8 110 Transcriptase (Thermo Scientific #18064014) and random hexamer primers (Roche
9
10 111 #11034731001) were used. The resulting cDNA was then added to a PCR reaction mix which
11
12 112 further consisted of Jumpstart Ready Mix (Sigma P2893) and exon-exon junction spanning
13
14 113 CamKII primers (FW TCCAACATTGTACGCCTCCAT; RV TGTTGGTGCTGTCGGAAGAT).
15
16 114 From all cDNA samples a fragment of the expected size could be amplified, suggesting that the
17
18 115 RNA samples contained pure RNA of sufficient integrity. All RNA samples thus passed our quality
19
20 116 control criteria and were subjected to RNA sequencing.
21
22
23

24 117

25 26 118 *RNA sequencing*

27
28 119 RNA sequencing was conducted at the Genomics Core Facility of the EMBL, Heidelberg,
29
30 120 Germany [\[RRID:SCR_004473\]](#). The cDNA library was generated using the non-stranded
31
32 121 NEBNext Ultra RNA Library Preparation Kit for Illumina (New England Biolabs, catalogue
33
34 122 #E7530), which includes oligo-dT bead selection of mRNA. For library enrichment, 13-14 PCR
35
36 123 cycles were performed. Pooled libraries were sequenced on the Illumina NextSeq 500 instrument
37
38 124 [\[RRID:SCR_014983\]](#) in a 75bp paired-end mode using High output flow cells.
39
40
41

42 125

43 44 126 **Data validation and quality control**

45
46 127 Sequencing read quality was assessed using FastQC (Babraham Bioinformatics)
47
48 128 [\[RRID:SCR_014583\]](#), the results of which were merged using MultiQC (<http://multiqc.info>)
49
50 129 [\[RRID:SCR_014982\]](#). Results are displayed in **Figure 2**. Per base quality *phred* scores range
51
52 130 from 34.80 to 35.15, indicating base call accuracies of >99.9% (**Figure 2A**). Overall 91.48-94.03%
53
54 131 of reads had a mean *phred* score of 30 or above (**Figure 2B**). In line with these scores, per base
55
56 132 N content (i.e. percentage of bases that could not confidently called) was very low, with a
57
58 133 maximum value 0.053%.
59
60
61
62
63
64
65

1
2
3
4 134
5
6 135
7
8
9 136
10
11 137
12
13 138
14
15 139
16
17 140
18
19 141
20
21 142
22
23 143
24
25 144
26
27 145
28
29 146
30
31 147
32
33 148
34
35 149
36
37 150
38
39 151
40
41 152
42
43 153
44
45 154
46
47 155
48
49 156
50
51 157
52
53 158
54
55 159
56
57
58
59
60
61
62
63
64
65

Figure 2 is about here

Reads were then mapped to the mm10 reference genome using STAR [5] [\[RRID:SCR_005622\]](#), which uniquely mapped between 39,000,000 and 59,000,000 reads, constituting an average 90.15% unique map rate across samples (**Figure 2D**). Since the library preparation protocol entails a PCR enrichment step, which can lead to technical duplication and hence an overestimation of observed transcripts, we used Seqmonk (Babraham Bioinformatics) [\[RRID:SCR_001913\]](#) to plot the read density against the duplication levels (i.e. the percentage of duplicate reads) for each transcript. The obtained duplication plots showed a clear positive relation between read density and duplication levels (**Figure 3** and **Supplemental Figure 1**), suggesting that the origin of read duplication is biological, rather than technical. Based on the above quality control measures we determined that our RNA-sequencing data was of sufficient quality to be used in downstream analyses, therefore we continued with gene expression analysis.

Figure 3 is about here

Analysis of gene expression

Using a 2 read cut-off we identified 16,900 to 17,600 transcripts per sample (**Figure 4A**). Raw gene counts can be found online (see Supporting Data – DOI to appear). Differential gene expression analyses across groups were performed using EdgeR v3.12.1 [6, 7] [\[RRID:SCR_012802\]](#) using only genes with a count per million (CPM) >1 in at least 4 samples (**Supplementary Table 1** for details on the commands used). Since laminar identity is an important feature of our experimental setup, we assessed the relative expression of known

1
2
3
4 160 molecular markers for L2/3 (*Cacna1h*, *Id2*, *Igfbp4*, *Igfn1*, *Mdga1*, *Plcx1*, *Rasgrf2*, *Rgs8*, *Tle3*)
5
6 161 and L4 (*Cartpt*, *Cyp39a1*, *Kcnh5*, *Kcnip2*, *Lmo3*, *Rorb*, *Scnn1a*) [8–10], which showed selective
7
8 162 enrichment of the laminar markers in isolated layers (**Figure 4B**).

10
11 163
12
13 164 *Figure 4 is about here*

14
15 165
16
17 166 To assess the variance in transcript counts, we calculated the coefficient of variation (CV) for
18
19 167 each transcript with a cut-off of 50 as the minimal read count separately for each group (**Figure**
20
21 168 **4C**). This analysis showed that, on average, 85.93% of transcripts have a CV below 15%,
22
23 169 suggesting low variance across transcript counts for individual genes. Principal component
24
25 170 analysis (PCA) showed that samples cluster based on layer, and the first two components
26
27 171 explained ~88% variance the data (**Figure 4C, Supplemental Figure 2B**).

28
29 172
30
31 173 These quality control routines suggest that we have obtained RNA-sequencing data of high read
32
33 174 quality, with individual bases being called confidently throughout the length of reads, which
34
35 175 uniquely map to the mm10 reference genome at high rates (>90% average). The laminar origin
36
37 176 of our samples could be identified through known molecular markers, confirming our samples are
38
39 177 of high anatomical specificity.
40
41
42
43

44 178 45 46 179 **Re-use potential**

47
48
49 180 The current RNA-seq dataset might help address the molecular underpinnings of cortical
50
51 181 experience-dependent plasticity. For example, it could be used (1) to identify genes whose
52
53 182 transcription is modulated in an experience-dependent manner, (2) to statistically map the
54
55 183 transcriptional networks at laminar resolution, (3) creating synergy with the single neuron RNA-
56
57 184 seq datasets [11, 12], to address the molecular diversity of the cortical networks, (4) combined
58
59 185 with the proteomic analysis performed under comparable experimental conditions in the
60
61
62
63
64
65

1
2
3
4
5
6
7
8
9
10
11
12
13
14
15
16
17
18
19
20
21
22
23
24
25
26
27
28
29
30
31
32
33
34
35
36
37
38
39
40
41
42
43
44
45
46
47
48
49
50
51
52
53
54
55
56
57
58
59
60
61
62
63
64
65

186 accompanying manuscript (Kole et al, submitted), to systematically study the transcriptional and
187 translational regulation of the genome upon altered sensory experience, and finally (5) to identify
188 and quantify splice isoforms, given the sequencing depth of the current dataset. Since splicing
189 and other posttranscriptional mechanisms govern which proteins are ultimately produced,
190 combining the current transcriptomic dataset with a proteomics approach would also be of high
191 importance.

192
193 The current dataset focuses on isolated cortical columns and layers, which are necessarily
194 diverse samples containing neuronal and non-neuronal cell classes. In terms of experience
195 dependent plasticity, although most previous studies focus on excitatory projections, inhibitory
196 cells and even non-neuronal cells have been implicated in plasticity [13–15]. This heterogeneity
197 might be particularly important for L2/3, as also shown by the principal component analysis
198 (**Figure 4D**), given the relative diversity of cellular populations in supragranular layers and their
199 heterogeneous connectivity patterns [16].

200
201 Researchers reusing our dataset should be aware that comparisons between control column C
202 and spared columns (A/E, B/D) may have to be approached with caution, as this would involve
203 two different columnar identities (whose transcriptomic dissimilarities are currently unknown),
204 each coming from cortices that have had different sensory experience. However direct
205 comparisons between the C columns across experimental conditions (i.e control versus deprived)
206 as well as within-animal across-column comparisons in deprived animals control for these
207 confounding variables.

208
209 Taken together we hope that this data will prove useful in discovering novel molecular targets
210 responsible for cortical plasticity and will lead to targeted control of plasticity in health and disease.

211

References

1. Hand PJ (1892) Plasticity of the rat cortical barrel system. In: Strick P, Morrison AD (eds) *Changing concepts of the nervous system*. Academic Press, New York, pp 49–75
2. Allen CB, Celikel T, Feldman DE (2003) Long-term depression induced by sensory deprivation during cortical map plasticity in vivo. *Nat Neurosci* 6:291–9. doi: 10.1038/nn1012
3. Celikel T, Szostak VA, Feldman DE (2004) Modulation of spike timing by sensory deprivation during induction of cortical map plasticity. *Nat Neurosci* 7:534–41. doi: 10.1038/nn1222
4. Clem RL, Celikel T, Barth AL (2008) Ongoing in vivo experience triggers synaptic metaplasticity in the neocortex. *Science* 319:101–4. doi: 10.1126/science.1143808
5. Dobin A, Davis CA, Schlesinger F, Drenkow J, Zaleski C, Jha S, Batut P, Chaisson M, Gingeras TR (2013) STAR: ultrafast universal RNA-seq aligner. *Bioinformatics* 29:15. doi: 10.1093/bioinformatics/bts635
6. Robinson MD, McCarthy DJ, Smyth GK (2010) edgeR: a Bioconductor package for differential expression analysis of digital gene expression data. *Bioinformatics* 26:139. doi: 10.1093/bioinformatics/btp616
7. McCarthy DJ, Chen Y, Smyth GK (2012) Differential expression analysis of multifactor RNA-Seq experiments with respect to biological variation. *Nucleic Acids Res* 40:4288. doi: 10.1093/nar/gks042
8. Molyneaux BJ, Goff LA, Rinn JL, Arlotta P (2015) Genome-wide Analysis of In Vivo Transcriptional Dynamics during Pyramidal Neuron Fate Selection in Neocortex *NeuroResource DeCoN: Genome-wide Analysis of In Vivo Transcriptional Dynamics during Pyramidal Neuron Fate Selection in Neocortex*. 275–288.
9. Xue M, Atallah B V., Scanziani M (2014) Equalizing excitation–inhibition ratios across visual cortical neurons. *Nature* 511:596–600. doi: 10.1038/nature13321
10. Rowell JJ, Mallik AK, Dugas-Ford J, Ragsdale CW (2010) Molecular analysis of neocortical layer structure in the ferret. *J Comp Neurol* 518:3272–3289. doi: 10.1002/cne.22399
11. Zeisel A, Munoz-Manchado AB, Codeluppi S, Lonnerberg P, La Manno G, Jureus A, Marques S, Munguba H, He L, Betsholtz C, Rolny C, Castelo-Branco G, Hjerling-Leffler J, Linnarsson S (2015) Cell types in the mouse cortex and hippocampus revealed by single-cell RNA-seq. *Science* (80-) 347:1138–1142. doi: 10.1126/science.aaa1934
12. Tasic B, Menon V, Nguyen TN, Kim TK, Jarsky T, Yao Z, Levi B, Gray LT, Sorensen SA, Dolbeare T, Bertagnolli D, Goldy J, Shapovalova N, Parry S, Lee C, Smith K, Bernard A, Madisen L, Sunkin SM, Hawrylycz M, Koch C, Zeng H (2016) Adult mouse cortical cell taxonomy revealed by single cell transcriptomics. *Nat Neurosci* 19:335–346. doi: 10.1038/nn.4216
13. Tropea D, Van Wart A, Sur M (2009) Molecular mechanisms of experience-dependent plasticity in visual cortex. *Philos Trans R Soc Lond B Biol Sci* 364:341–55. doi: 10.1098/rstb.2008.0269
14. Kole K (2015) Experience-dependent plasticity of neurovascularization. *J Neurophysiol* 114:2077–9. doi: 10.1152/jn.00972.2014
15. Foeller E, Celikel T, Feldman DE (2005) Inhibitory sharpening of receptive fields contributes to whisker map plasticity in rat somatosensory cortex. *J Neurophysiol* 94:4387–400. doi: 10.1152/jn.00553.2005
16. Markram H, Muller E, Ramaswamy S, Reimann MW, Abdellah M, Sanchez CA, Ailamaki A, Alonso-Nanclares L, Antille N, Arsever S, Kahou GAA, Berger TK, Bilgili A, Buncic N, Chalimourda A, Chindemi G, Courcol J-D, Delalondre F, Delattre V, Druckmann S, Dumusc R, Dynes J, Eilemann S, Gal E, Gevaert ME, Ghobril J-P, Gidon A, Graham JW, Gupta A, Haenel V, Hay E, Heinis T, Hernando JB, Hines M, Kanari L, Keller D, Kenyon

1
2
3
4
5
6
7
8
9
10
11
12
13
14
15
16
17
18
19
20
21
22
23
24
25
26
27
28
29
30
31
32
33
34
35
36
37
38
39
40
41
42
43
44
45
46
47
48
49
50
51
52
53
54
55
56
57
58
59
60
61
62
63
64
65

263 J, Khazen G, Kim Y, King JG, Kisvarday Z, Kumbhar P, Lasserre S, Le Bé J-V,
264 Magalhães BRC, Merchán-Pérez A, Meystre J, Morrice BR, Muller J, Muñoz-Céspedes
265 A, Muralidhar S, Muthurasa K, Nachbaur D, Newton TH, Nolte M, Ovcharenko A,
266 Palacios J, Pastor L, Perin R, Ranjan R, Riachi I, Rodríguez J-R, Riquelme JL, Rössert
267 C, Sfyarakis K, Shi Y, Shillcock JC, Silberberg G, Silva R, Tauheed F, Telefont M, Toledo-
268 Rodriguez M, Tränkler T, Van Geit W, Díaz JV, Walker R, Wang Y, Zaninetta SM,
269 DeFelipe J, Hill SL, Segev I, Schürmann F (2015) Reconstruction and Simulation of
270 Neocortical Microcircuitry. *Cell* 163:456–492. doi: 10.1016/j.cell.2015.09.029
271

1
2
3
4
5
6
7
8
9
10
11
12
13
14
15
16
17
18
19
20
21
22
23
24
25
26
27
28
29
30
31
32
33
34
35
36
37
38
39
40
41
42
43
44
45
46
47
48
49
50
51
52
53
54
55
56
57
58
59
60
61
62
63
64
65

272 Availability of the supporting data

273 Supporting data are available online (<https://goo.gl/tBof51>) and will be distributed via GigaScience
274 DB.

275 Raw sequence reads were deposited in NCBI GEO.

276 Link: <https://www.ncbi.nlm.nih.gov/geo/query/acc.cgi?acc=GSE90929>

278 List of abbreviations

279 EDP Experience dependent plasticity

280 L2/3 Cortical Layer 2/3, also known as supragranular layers

281 L4 Cortical Layer 4, i.e. granular layer

283 Competing interests

284 The authors declare no competing interests.

286 Author contributions

287 KK performed all experimental manipulations, sample acquisition, biological and bioinformatic
288 quality controls, and prepared the tables and figures. YK and JaP performed bioinformatic
289 analysis. JeP performed library prep. VB supervised RNA-seq. PT contributed bioinformatic
290 analysis and co-supervised the project. TC designed and supervised the project. KK and TC wrote
291 the manuscript. All authors edited otherwise approved the final version of the manuscript.

1
2
3
4 **292 Figure Legends**

5 **293**
6 **294** **Figure 1.** Overview of the experimental design, sample collection and data organization. **(A)** Pups
7 **295** were bilaterally spared or deprived of off their C-row whiskers between P12 and P23-P24, when
8 **296** acute slices are made and column- and layer-specific tissues were excised. **(B)** RNA was isolated,
9 **297** checked for integrity and purity, and subsequently sequenced. **(C)** Organization of the database.
10 **298** Colour codes denote experimental groups. Same denominations are used in the read counts
11 **299** matrix file (see **Supplemental Data**).
12
13
14

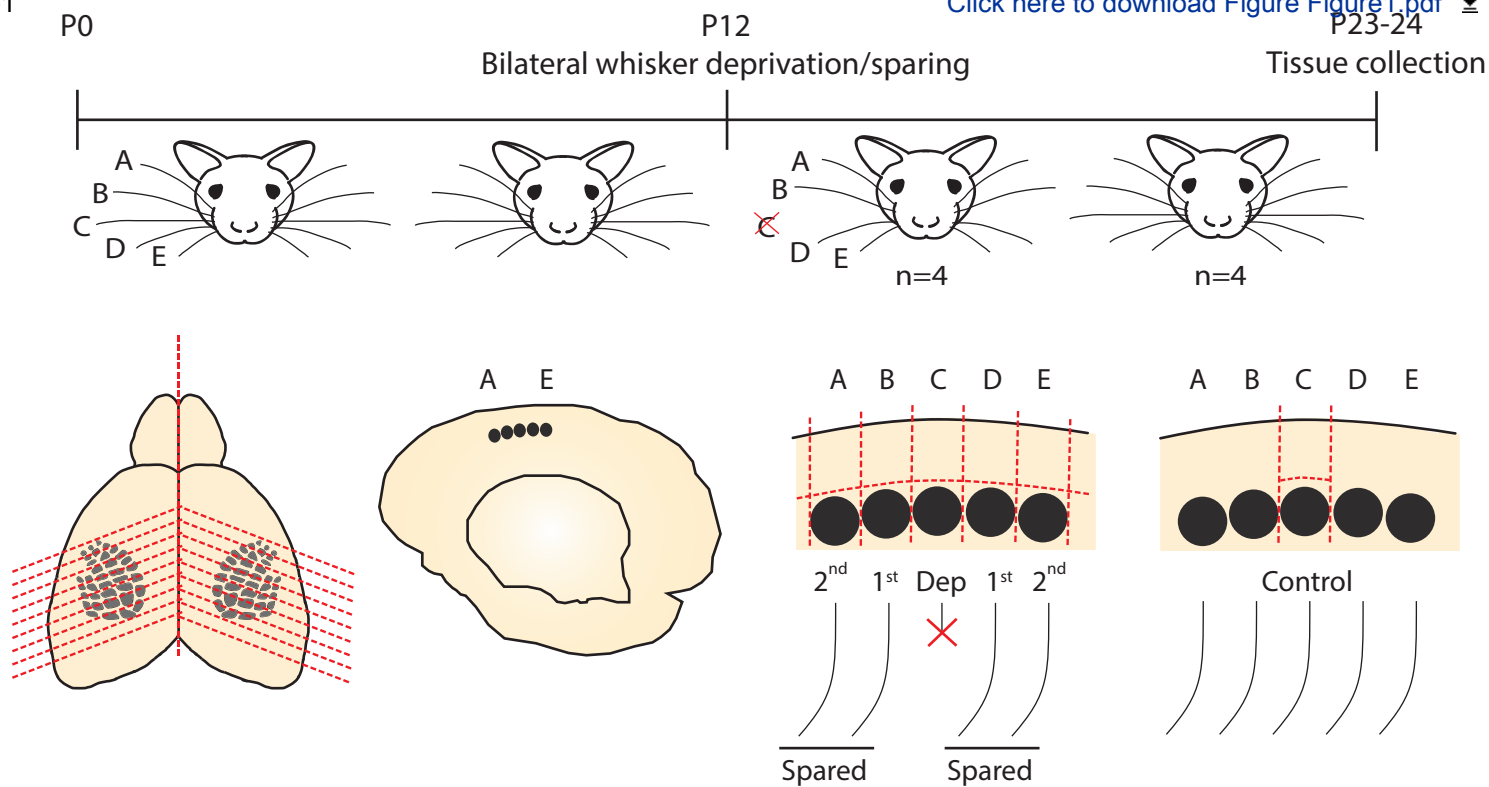
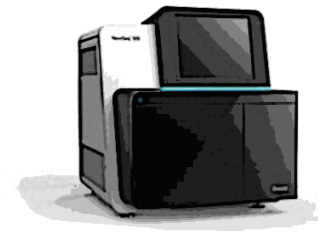
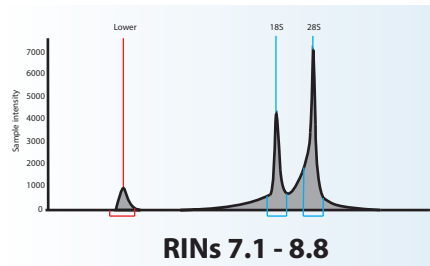
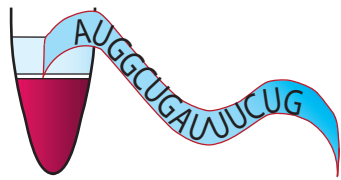
15 **300**
16 **301** **Figure 2.** FastQC and STAR output graphs for all samples. **(A-B)** *Phred* scores per base and
17 **302** per sequence. **(C)** Per sequence GC content. **(D)** STAR output of alignment scores.
18 **303**

19 **304** **Figure 3.** Overlays of duplication plot contours, showing a positive correlation between read
20 **305** density and duplication levels. Depicted contours enclose 90% of the data points.
21 **306**

22 **307** **Figure 4.** Gene expression analyses. **(A)** Histogram of read counts per transcript per sample.
23 **308** With a cut-off of 2 reads, between 16,900 and 17,600 transcripts could be identified across
24 **309** samples. **(B)** Relative expression of known molecular markers for cortical laminae. Layer 4
25 **310** markers are enriched in samples originating from this layer; the same is true for Layer 2/3 marker
26 **311** expression in Layer 2/3 samples. **(C)** Cumulative plots of the coefficient of variance (CV) of
27 **312** individual experimental groups. Including only transcripts identified by 50 reads or more, average
28 **313** CVs of <15% are found in ~85% of transcripts. **(D)** Principal component analysis (PCA) showing
29 **314** sample clustering by layer, including only transcripts identified by at least 50 reads. Principal
30 **315** component (PC) 1 and 2 account for 88% of overall variance.
31 **316**

32 **317** **Supplemental Figure 1.** Duplication plots for all samples, produced using SeqMonk (Babraham
33 **318** Bioinformatics).
34 **319**

35 **320** **Supplemental Figure 2.** **(A)** Cumulative plots of the coefficient of variance (CV) of experimental
36 **321** each group, including transcripts identified by at least one read. Average CVs of <25% are
37 **322** found in ~85% of transcripts. **(B)** Principal component analysis (PCA) including transcripts
38 **323** identified by at least one read. The majority (88%) of overall variance is explained by Principal
39 **324** components (PC) 1 and 2.
40
41
42
43
44
45
46
47
48
49
50
51
52
53
54
55
56
57
58
59
60
61
62
63
64
65

**B**

RNA isolation, quality control and sequencing

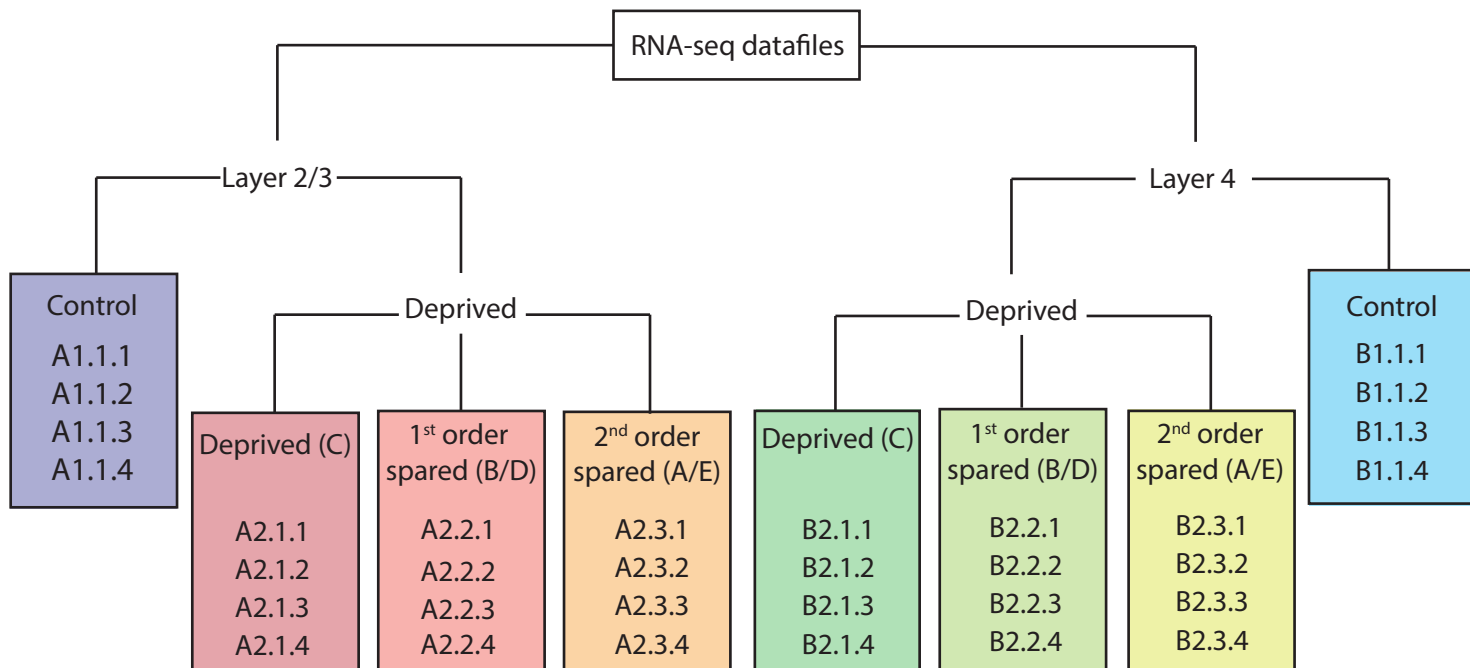
C

Figure2

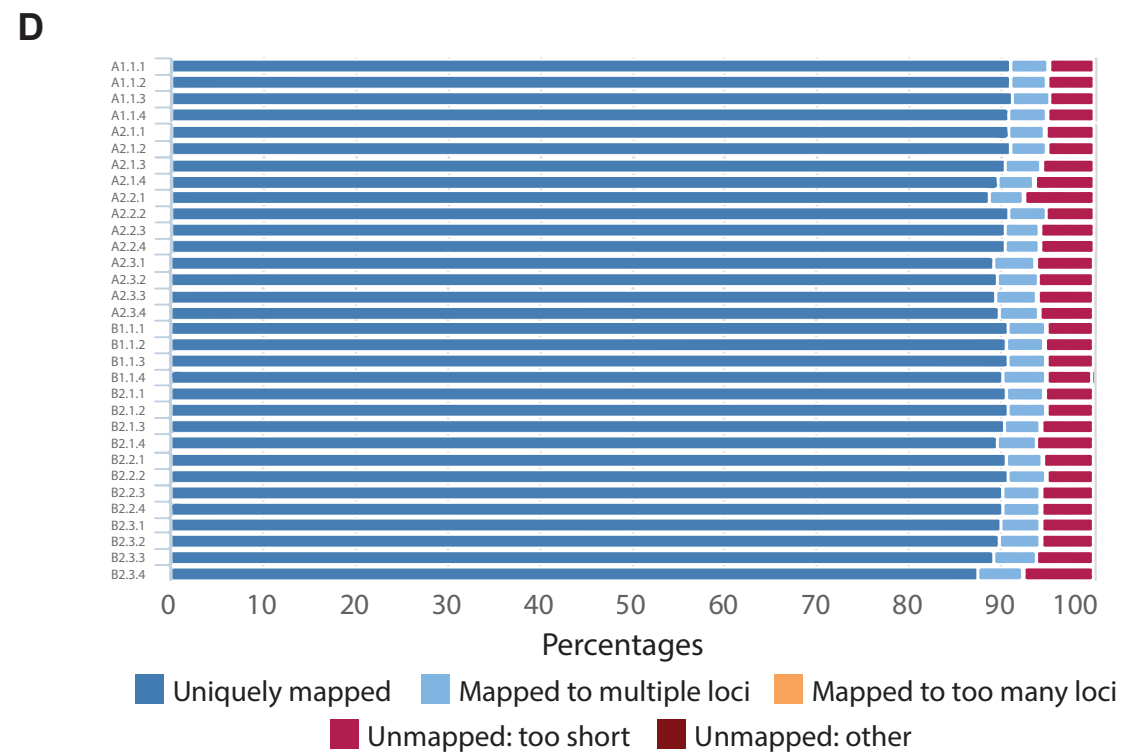
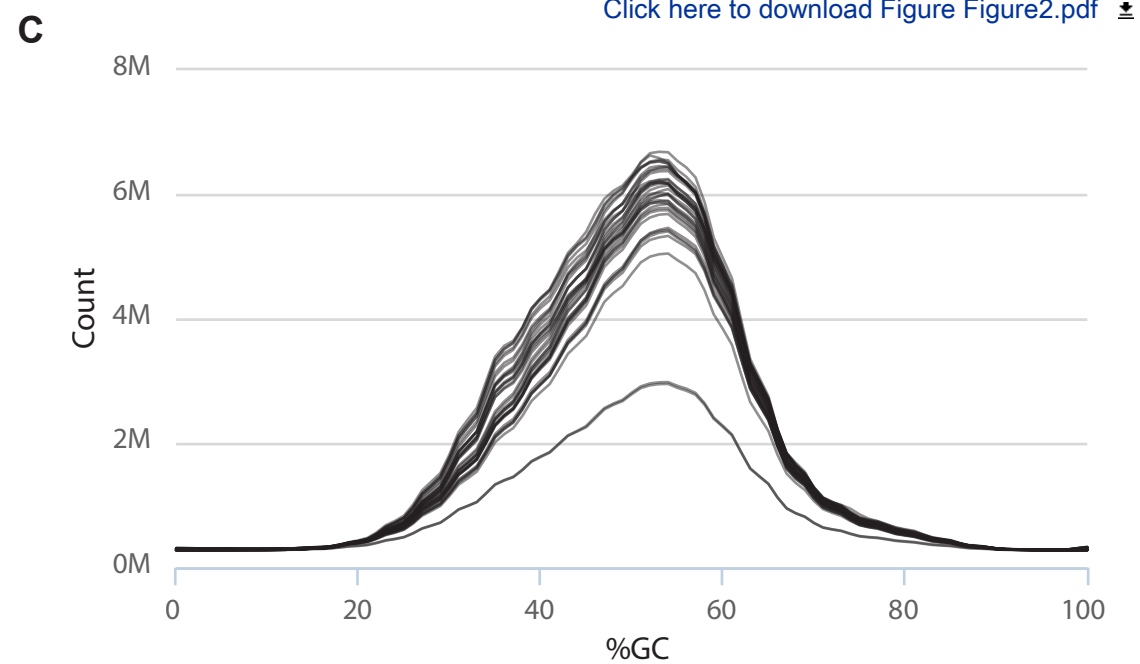
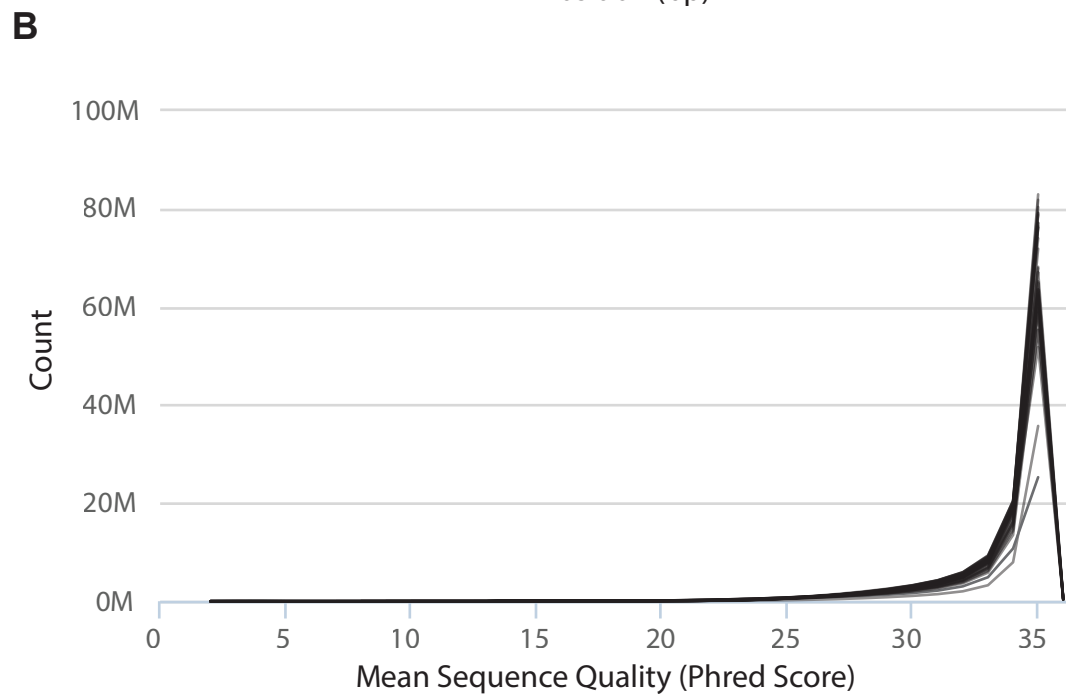
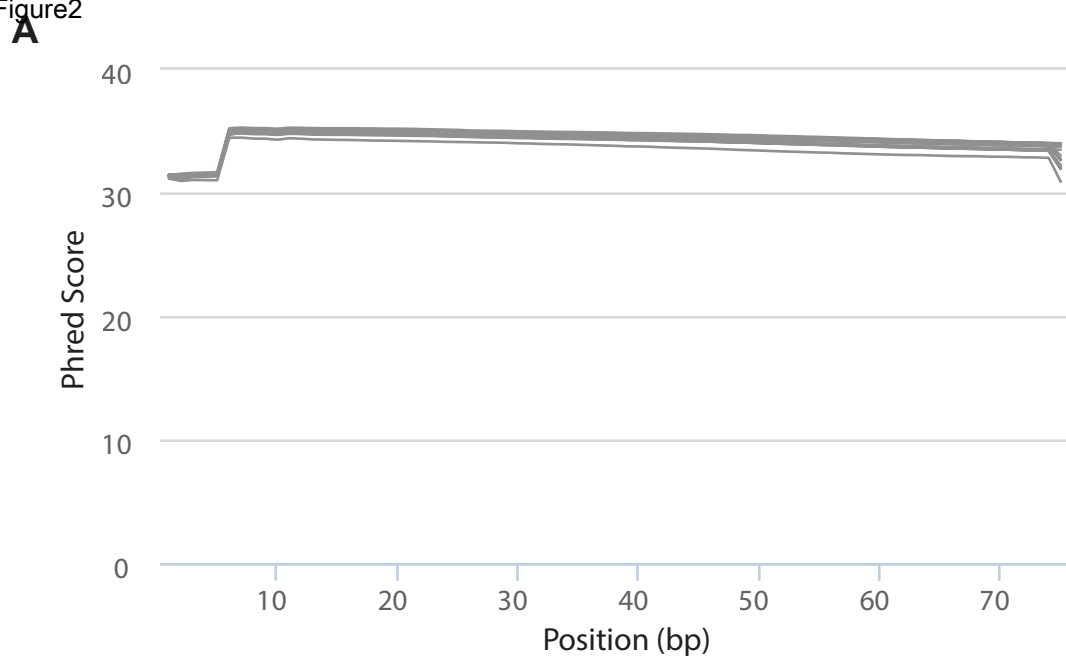


Figure3

[Click here to download Figure Figure3.pdf](#)

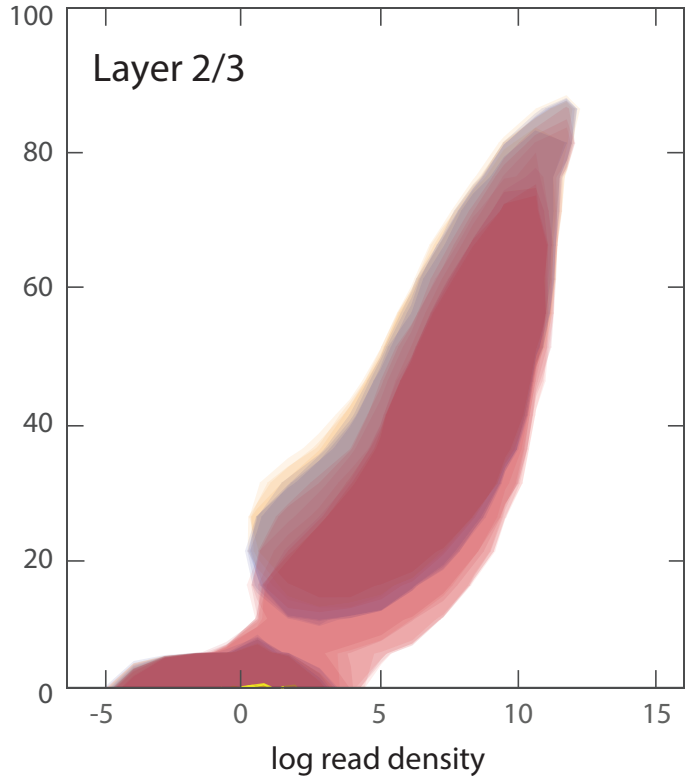
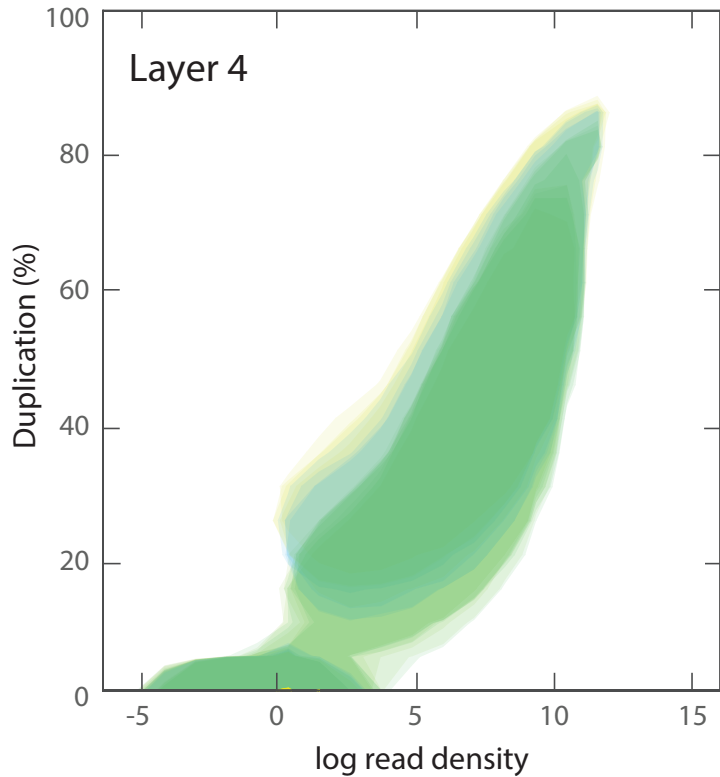
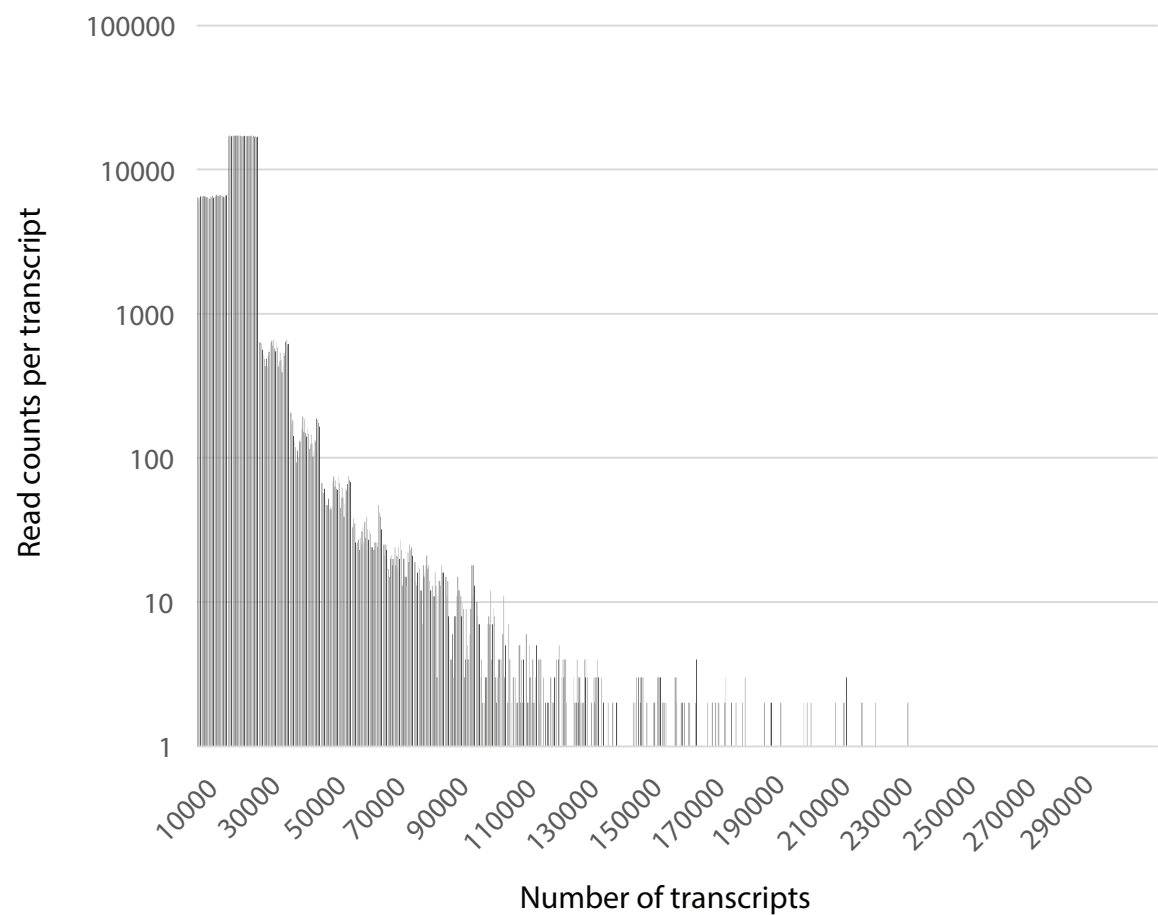
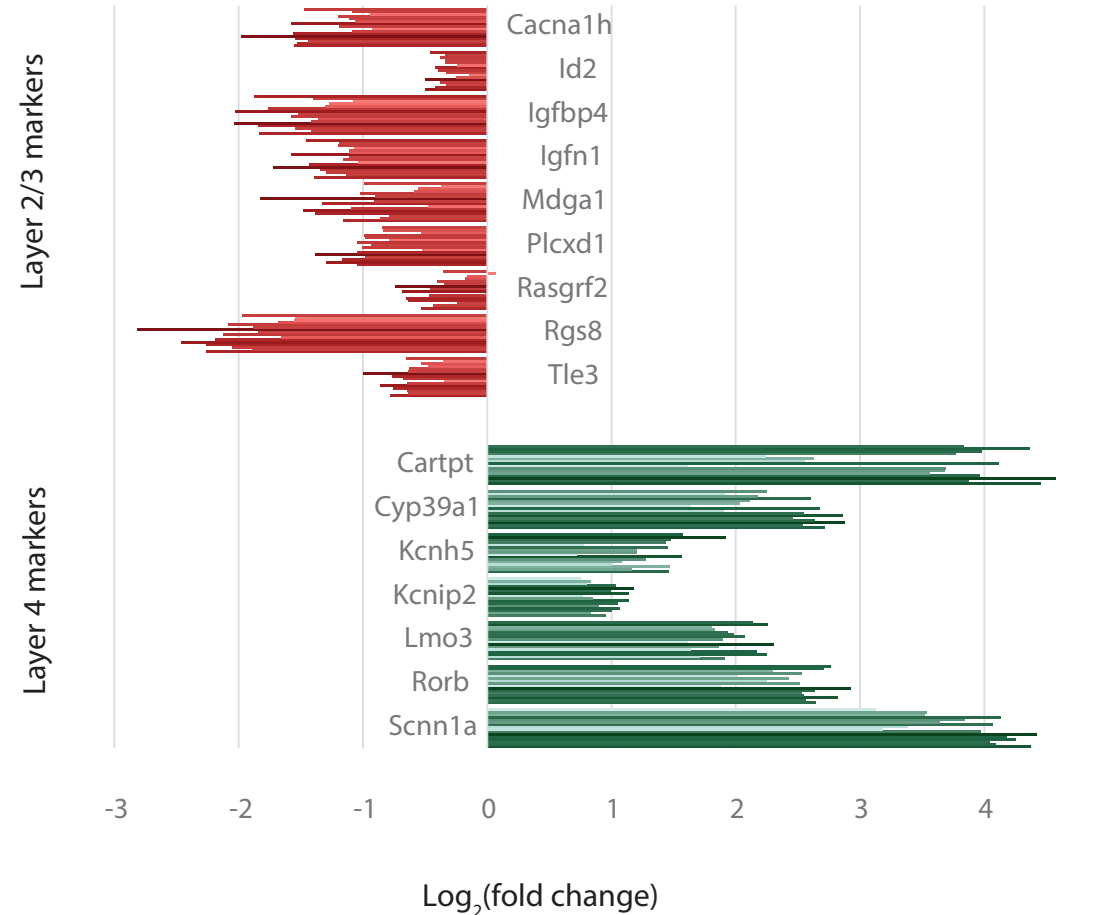
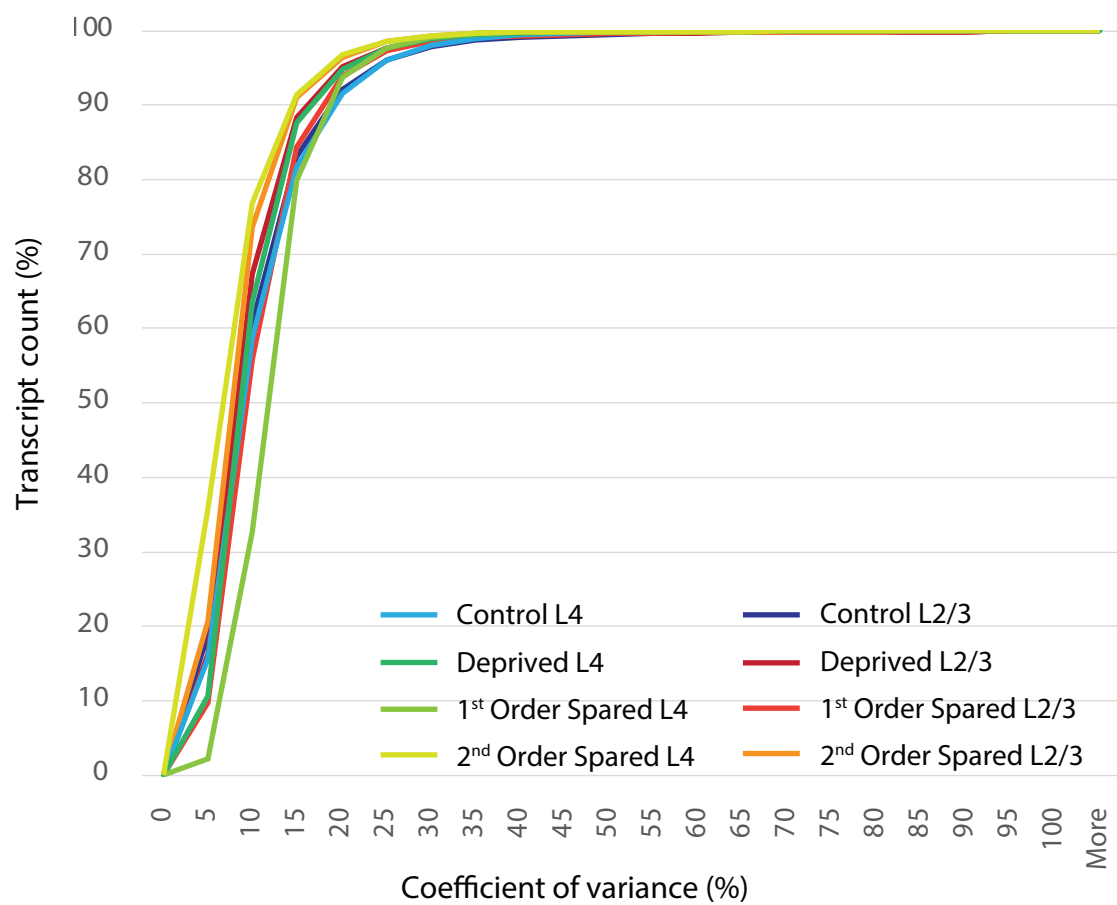
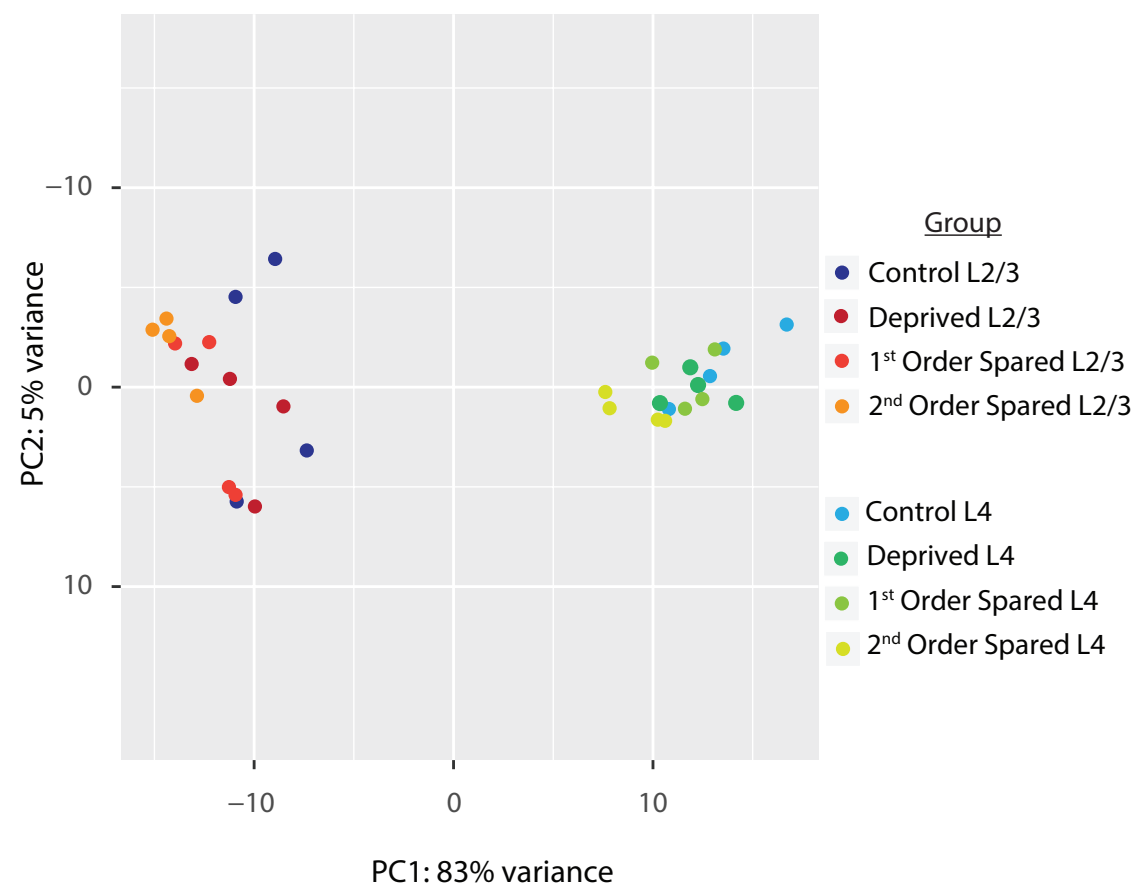


Figure 4

[Click here to download Figure Figure_4.pdf](#)**A****B****C****D**



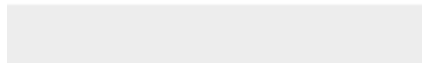




[Click here to access/download](#)

Supplementary Material

[Supplementary_Table1_EdgeRcommands.txt](#)





Click here to access/download

Supplementary Material

Gigascience_Kole_RevisedRound2.docx

